IET Control Theory & Applications

Research Article

IET Journals
The Institution of Engineering and Technology

Feedback control of oxygen uptake profiles during robotics-assisted treadmill exercise

ISSN 1751-8644
Received on 27th June 2014
Revised on 18th September 2014
Accepted on 15 October 2014
doi: 10.1049/iet-cta.2014.0725
www.ietdl.org

Matthias Schindelholz[1,2] ✉, *Kenneth J. Hunt*[1,2]

[1] *Institute for Rehabilitation and Performance Technology, Division of Mechanical Engineering, Department of Engineering and Information Technology, Bern University of Applied Sciences, CH-3400 Burgdorf, Switzerland*
[2] *Reha Rheinfelden, CH-4310 Rheinfelden, Switzerland*
✉ *E-mail: matthias.schindelholz@bfh.ch*

Abstract: Gait rehabilitation robots have potential for cardiovascular rehabilitation of patients with neurological deficits. A novel method was developed to guide exercise intensity by feedback control of oxygen uptake rate with a focus on tracking ramps as typically applied in maximal exercise testing. This approach is important as prior observations have noted a non-linear oxygen uptake response to increasing work rate, whereas a linear progression of exercise intensity is desirable. The proposed oxygen-uptake controller has embedded within it a human-in-the-loop feedback system for control of mechanical work rate which takes its target work rate from the automatic oxygen uptake control loop. Results of step and ramp tracking of target oxygen-uptake profiles, and disturbance rejection tests, demonstrated the technical feasibility and accuracy of the approach. Comparison with open-loop tests demonstrated clearly that the feedback system linearises the oxygen-uptake response and that linear progression of exercise intensity leads to higher peak oxygen uptake values. Further work will focus on clinical feasibility and the potential for cardiovascular rehabilitation in patients with neurological deficits.

Nomenclature

HR	heart rate
P_{raw}	unfiltered total mechanical work rate
P_{total}	low pass filtered total mechanical work rate
$P_{passive}$	passive mechanical work rate (constant value), estimated in passive test
P_{mech}	active mechanical work rate, $P_{mech} = P_{total} - P_{passive}$
$P_{mech\ peak}$	peak active mechanical work rate
P^*_{mech}	target mechanical work rate
$\dot{V}O_2$	rate of oxygen uptake
$\dot{V}O_{2\ peak}$	peak oxygen uptake rate
$\dot{V}O_{2\,max}$	maximal value of oxygen uptake rate, only achieved if the oxygen uptake rate reaches plateau
$\dot{V}O^*_2$	target rate of oxygen uptake
$\dot{V}O_{2(sim)}$	simulated oxygen uptake with the linear first order plant model P_0
$\dot{V}CO_2$	rate of carbon dioxide output
root mean square error	$RMSE = \sqrt{\left(\sum_{i=1}^{N}(x_i - x_{target,i})^2\right)/N}$ x corresponds to the variable; N corresponds to the number of samples over a specified time range. This is a frequently used indicator of the differences between predicted values by a model and the values actually observed.
$RMSE(P_{mech} \leftrightarrow P^*_{mech})$	RMSE between actual and target mechanical work rate
$RMSE(\dot{V}O_2 \leftrightarrow \dot{V}O_{2(sim)})$	RMSE between actual and simulated oxygen uptake rate
$RMSE(\dot{V}O_2 \leftrightarrow \dot{V}O^*_2)$	RMSE between actual and target oxygen uptake rate
$\dot{V}O_2$-work rate relationship	oxygen uptake rate per work rate relationship: $(\dot{V}O_{2\ peak}/P_{mech\ peak})$
M	moment of force (torque)
ω	angular speed
BWS	body weight support
RATE	robotics-assisted treadmill exercise
IET	incremental exercise test

1 Introduction

Robotic devices for gait rehabilitation have primarily been applied for recovery of walking function and adaptation of the central nervous system in individuals with sundry neurological deficits [1, 2]. In the recent past, cardiovascular rehabilitation has increased in importance as a complementary application of such devices [3–7]. Robotics-assisted treadmill exercise (RATE) provides the potential to evaluate and train exercise capacity in individuals with serious neurological impairments [4, 8–10]. A satisfactory level of cardiovascular fitness supports better management of the condition and better performance in the activities of daily living [11]. However, a study with stroke patients using the Lokomat gait rehabilitation robot showed that exercise intensity did not reach recommended levels for aerobic training during RATE [12], regardless of the Lokomat device settings. This raises the question of how to specify and control exercise intensity to achieve a training effect.

It has been shown that feedback control of heart rate profiles in RATE is technically feasible [13], thus providing one means of controlling the subjects' effort. Other work has examined different intensity-related variables including external mechanical work rate, oxygen uptake, ratings of perceived exertion, human metabolic work rate and different walking conditions [7, 9, 14–17]. In the

field of exercise physiology, it is recommended that the intensity of training sessions be specified through oxygen uptake rate ($\dot{V}O_2$) [18, 19] since $\dot{V}O_2$ gives the most reliable and direct indication of total exercise intensity in the human body. Oxygen uptake is the gold standard for assessment of aerobic fitness and the optimal variable for precise control of training intensity [20].

It has previously been shown that feedback control of oxygen uptake during RATE is feasible for step tracking tasks in able-bodied subjects [15]. The design of feedback controllers for tracking of $\dot{V}O_2$ ramp profiles has been predicted theoretically and evaluated in simulation [21]. A method for estimating maximal aerobic capacity would be an important contribution to the design of fitness training and assessment protocols for RATE. A well-established method is incremental exercise testing (IET), where the exercise intensity should be increased rampwise until the subject reaches the limit of functional capacity. It has been shown that oxygen uptake responses are not linearly coupled with the work rate during RATE [22], presumably because unmeasured components of work increase disproportionately at higher intensity. Closed loop control of oxygen uptake would provide a method of compensating for such non-linearities and also for plant disturbances (e.g. speed changes) and population diversity. Further, we hypothesize that approaching the limit of functional capacity in a linear fashion, (by means of feedback control of $\dot{V}O_2$) may lead to higher peak oxygen uptake values.

The present work extends the idea of direct feedback control of oxygen uptake profiles for RATE to ramp tracking. The controller is embedded within a human-in-the-loop feedback structure

Fig. 1 *Experimental Setup*

User with breath-by-breath cardiorespiratory monitoring system performs a feedback task on the Lokomat

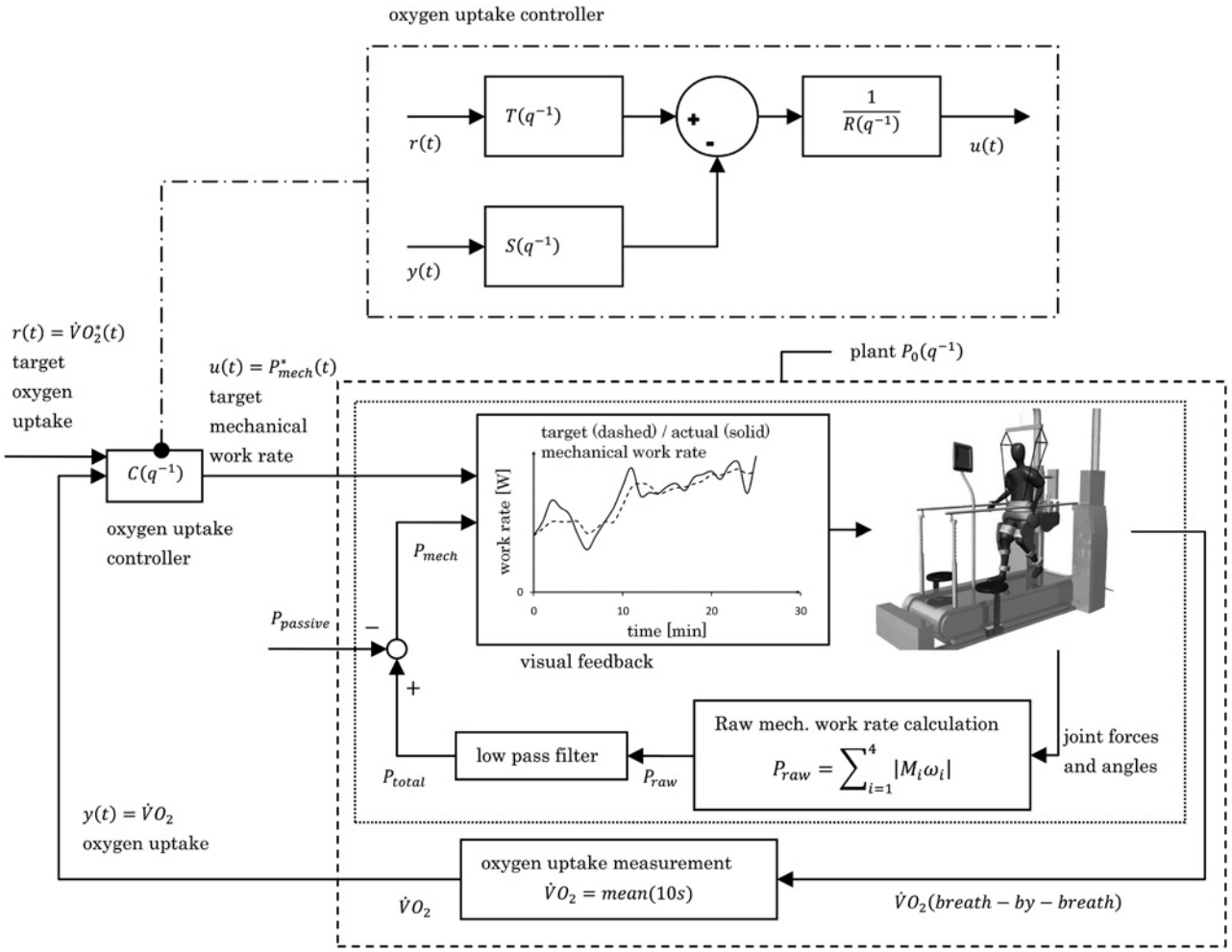

Fig. 2 *Feedback control loop with controller structure*

Dash-dotted line: RST-structure of the controller
Dotted line: human-in-the-loop work rate control
M_i-moments of force; ω_i-angular speeds
Dashed line: open loop structure of the plant

to allow the subject to perform volitional control of mechanical work rate in a similar way to [13]. The software implementation of the approach was described in detail in recent work [23]. The feedback controller calculates the target mechanical work rate for the human in the loop, so that the desired target oxygen uptake rate is achieved. The actual mechanical work rate, which represents the effort of the subject and the target mechanical work rate are visualised to the subject using the biofeedback system.

The aim of the present work was to test the technical feasibility of the new method for feedback control of oxygen uptake rate during RATE with a special focus on ramp tracking. Two controllers (single and double integrator) were tested with step tracking, disturbance rejection and ramp tracking tasks and compared with open-loop control. We also aimed to investigate the non-linearity of the oxygen uptake response in RATE and the ability of the controller to linearise this key response; in this regard, the potential ability of feedback linearisation to promote higher peak oxygen uptake ($\dot{V}O_{2\ peak}$) and heart rate (HR) values was examined.

2 Materials and methods

2.1 Instrumentation and control strategy

We used the Lokomat gait orthosis system [LokomatPro version 5, Hocoma AG, Volketswil, Switzerland] with integrated treadmill

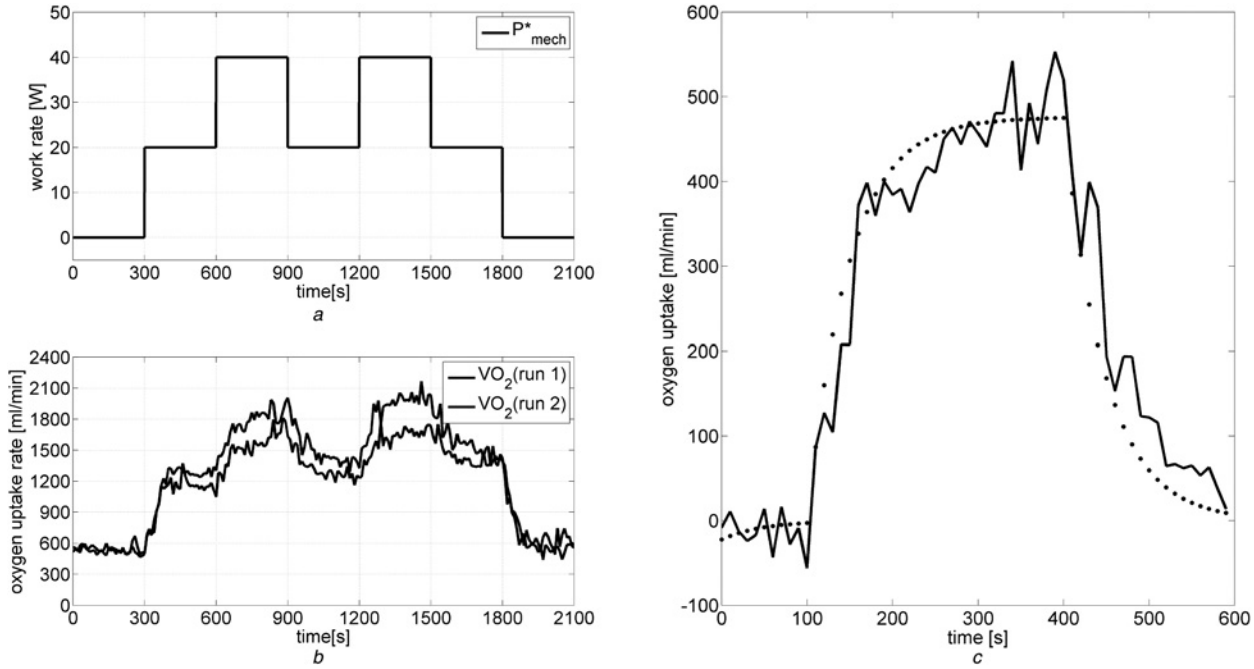

Fig. 3 *Identification data sets and simulated model output*

a Target mechanical work rate input signal
b Oxygen uptake rate output signal of both identification tests
c Identified first order nominal plant model $P_0(q^{-1})$ simulation and averaged signal of all four steps of the two tests (starting offset level subtracted)
The model fit value is 73.7%

Type	Controller	$\dot{V}O_2^*$ min. [ml/min]	$\dot{V}O_2^*$ max. [ml/min]	Section times [min]
Step tracking	$C1$	1200	1600	0-5-10-15-20-25
Disturbance rejection	$C1$	1400	1400	0-5-10-15-20-25
Open loop	none	P^* min.= 0W	P^* max.= 120W	0-5-15-20
Ramp tracking	$C1$	1000	3000	0-5-15-20
Ramp tracking delayed	$C1$	1000	3000	0-5-15-20
Ramp tracking	$C2$	1000	3000	0-5-15-20

Fig. 4 *Outcomes of the tests*

Note: Transient initial and final phases were neglected in calculating any RMSE values of oxygen uptake in this work
Start point of the calculation was always 300 s and end point was the final time value or the beginning of the final transient phase

[h/p/cosmos GmbH, Nussdorf-Traunstein, Germany.] and dynamic body weight support system [Lokolift, Hocoma AG.] (Fig. 1). An interface unit [Lokomaster Output Box, Hocoma AG.] provided force and angle sensor data from all four actuated joints (i.e. the hip and knee joints) to allow calculation of the subjects' active participation at the human machine interface points represented by the active mechanical work rate P_{mech} [23]. The raw mechanical work rate (20 Hz sampling frequency), denoted P_{raw}, was IIR low-pass filtered (first order, 0.02 Hz cutoff frequency) and the passive work rate P_{passive} was subtracted. P_{passive} was estimated prior the start of each test by taking the mean value of the total mechanical work rate P_{total} over a short time period during passive walking. The formula used to calculate the raw mechanical work rate was

$$P_{\text{raw}} = \sum_{i=1}^{4} |M_i \omega_i| \tag{1}$$

with moments of force M_i and angular speeds ω_i of hip and knee joints.

A manual human-in-the-loop feedback system was implemented (Fig. 2, dotted line) to allow the subject to volitionally control their external mechanical work rate. This provided visualisation of the target mechanical work rate P^*_{mech} and the actual mechanical work rate P_{mech} in a graph on a large screen in front of the treadmill (Fig. 1). The subject was instructed to adjust the forces they applied to the orthoses via the shank and thigh cuffs so as to keep P_{mech} close to P^*_{mech}.

Oxygen uptake ($\dot{V}O_2$) and carbon dioxide output ($\dot{V}CO_2$) were measured in real time using a breath-by-breath metabolic monitoring system [Metamax 3B, Cortex Biophysik GmbH, Leipzig, Germany]. The system was calibrated for volume and gas concentration using a volumetric syringe and a precision gas mixture, respectively, prior to each test. HR was measured using a HR belt [T31, Polar Electro, Kempele, Finland] and a receiver board [HRMI, Sparkfun, Boulder, Colorado, USA].

2.2 Plant identification procedure

In an identification procedure, two open loop step tests were performed to obtain the dynamic relationship between target mechanical work rate (input P^*_{mech}) and oxygen uptake (output $\dot{V}O_2$) under the assumption of a discrete linear time-invariant plant model $P_0(q^{-1})$, where q^{-1} is the delay operator (Figs. 3*a* and *b*). We assumed at the outset that the plant can be modelled by a mono-exponential (first-order) response, which is the usual assumption in exercise physiology [20]. Both tests were used for parameter estimation and model validation by taking the average of the four up-down step responses to create a single data set. During the identification tests, two target work rate levels of 20 and 40 W were applied in sequence for 5 min each (Fig. 3*a*). The estimated transfer function, obtained using a linear least-squares procedure, represents the nominal open-loop plant $P_0(q^{-1})$ (Fig. 3*c*) and is used for controller development. The sample time for identification was 10 s. The generic structure of the plant model is

$$A(q^{-1})y(t) = B(q^{-1})u(t) + e(t) \tag{2}$$

with A and B polynomials in the delay operator q^{-1} and output variable y, input variable u and disturbance e in time domain.

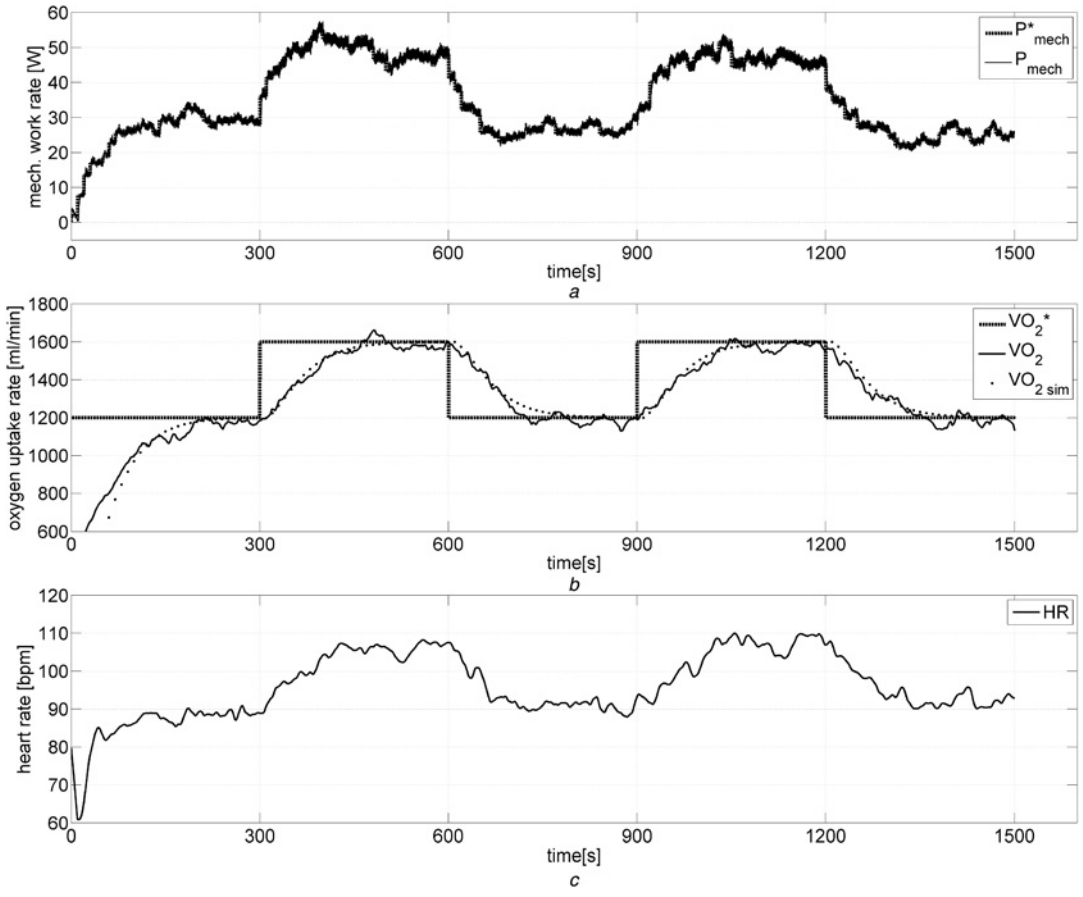

Fig. 5 *Step tracking with controller C_1*

a Target mechanical work rate P^*_{mech}, calculated by the controller based on $\dot{V}O_2^*$ and $\dot{V}O_2$; active mechanical work rate P_{mech} performed by the subject
b Target oxygen uptake rate $\dot{V}O_2^*$, oxygen uptake rate $\dot{V}O_2$ and simulated oxygen uptake rate $\dot{V}O_{2(\text{sim})}$ based on the plant model $P_0(q^{-1})$
c Heart rate HR

2.3 Controller development

The nested-loop feedback control structure consists of a human-in-the-loop work rate control inner loop, in conjunction with an outer-loop oxygen uptake feedback controller (Fig. 2). Two different $\dot{V}O_2$ controllers, denoted $C_1(q^{-1})$ and $C_2(q^{-1})$, were designed based on the open loop transfer function $P_0(q^{-1})$: C_1 has a single integrator and C_2 has a double integrator. Each feedback controller calculates the target mechanical work rate P^*_{mech} for the human-in-the-loop control part, based on the predefined target oxygen uptake $\dot{V}O_2^*$ and measured actual oxygen uptake $\dot{V}O_2$. The controllers were implemented using a standard structure for anti-reset windup in discrete-time controllers [24]. Each controller has the same generic structure (dash-dotted box in Fig. 2), that is

$$P^*_{\text{mech}}(t) = \frac{1}{R(q^{-1})}(T(q^{-1})\dot{V}O_2^*(t) - S(q^{-1})\dot{V}O_2(t)) \quad (3)$$

with R, S and T polynomials in the delay operator q^{-1}.

(1) C_1–*single integrator:* With a first-order plant model and a single integrator in the controller, that is, R included the factor $\Delta = 1 - q^{-1}$, three closed-loop poles had to be selected. A dominant pole pair was determined based on a desired 10–90% closed-loop rise time of 120 s and relative damping of 0.999 for the nominal closed-loop response of an equivalent second-order transfer function. The third pole was selected based on a first-order system, about three times faster than the dominant second-order poles with rise time of 36 s.

(2) C_2–*double integrator:* For delay-free tracking of a ramp target signal, the controller included an additional integrator, that is, the factor $(1 - q^{-1})^2$ was incorporated in R. For C_2, four closed-loop poles were specified, determined by selection of the rise time and relative damping for two second order transfer functions. The first pole pair had a rise time of 120 s and damping of 0.999, as for C_1. The second pole pair had a rise time of 186 s and a damping of 0.999. These design parameters were chosen such that the nominal closed loop sensitivity and complementary sensitivity functions had approximately the same bandwidths determined in the design of controller C_1. Both controllers were implemented in discrete time with a sample time of 10 s.

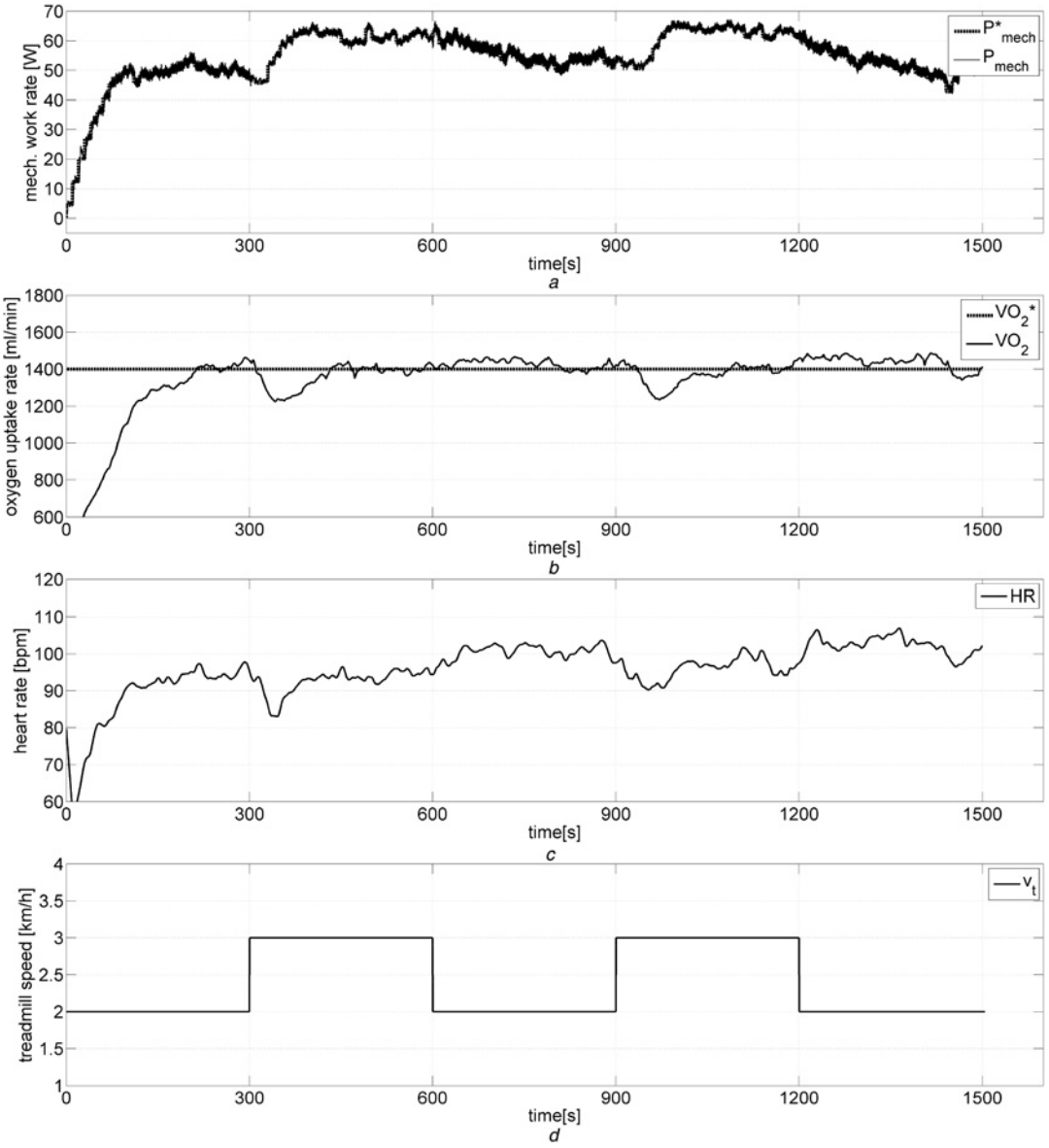

Fig. 6 *Disturbance rejection test with C_1 and periodical speed level changes*

a Target mechanical work rate P^*_{mech}, calculated by the controller based on $\dot{V}O_2^*$ and $\dot{V}O_2$; active mechanical work rate P_{mech} performed by the subject
b Constant target oxygen uptake rate $\dot{V}O_2^*$, oxygen uptake rate $\dot{V}O_2$
c Heart rate HR
d Treadmill speed v_t as disturbing variable

The input–output transfer function of the closed loop (Fig. 2) is

$$\frac{y(t)}{r(t)} = \frac{B(q^{-1})T(q^{-1})}{A(q^{-1})R(q^{-1}) + B(q^{-1})S(q^{-1})} \quad (4)$$

The pole placement method involves solving the characteristic equation for R and S [24]

$$A(q^{-1})R(q^{-1}) + B(q^{-1})S(q^{-1}) = \varphi_1(q^{-1})\varphi_2(q^{-1}) \quad (5)$$

where the desired closed-loop poles are set using the polynomials φ_1 (2 dominant poles for C_1 and C_2) and φ_2 (1 fast pole for C_1, two faster poles for C_2).

T is computed in the form $T(q^{-1}) = k\varphi_2(q^{-1})$, with k a constant, to cancel the faster poles φ_2 from the tracking response and to achieve unity steady-state gain overall

$$\frac{y(t)}{r(t)} = \frac{B(q^{-1})T(q^{-1})}{\varphi_1(q^{-1})\varphi_2(q^{-1})} = \frac{kB(q^{-1})}{\varphi_1(q^{-1})} \text{ with } k = \frac{\varphi_1(1)}{B(1)} \quad (6)$$

2.4 Testing protocols

Several tests were performed to assess control performance (Fig. 4). In each test the treadmill speed was set to 2 km/h, except in the disturbance rejection test where it was increased periodically to 3 km/h. Body weight support (BWS) was 30 kg in all tests. The single test person was a healthy, normal male aged 49 years (author K.J.H.), familiar with Lokomat walking. His mass was 83 kg and his height was 185 cm.

(1) *Step tracking:* During this test the target oxygen uptake was changed periodically between two different levels. The target oxygen uptake profile was specifically chosen in a range recommended for cardiovascular training. Exercise intensity should be above a minimal required intensity level to result in changes in physiologic parameters. The ACSM recommends a relative training intensity of 37 to 64% of $\dot{V}O_{2\,max}$ for deconditioned persons and 46 to 91% of $\dot{V}O_{2\,max}$ for normal able-bodied adults [19]. These target $\dot{V}O_2$ levels are similar to the range used in the identification procedure, which also lies within the recommended ranges.
(2) *Disturbance rejection:* The controller's objective in this test was to maintain a constant oxygen uptake rate. The treadmill speed changed every 5 min between 2.0 km/h and 3.0 km/h to investigate the disturbance rejection abilities of the controller.
(3) *Open loop:* The aim of this test was to investigate the degree of linearity of the oxygen uptake response to a linearly-increasing target work rate profile, that is, no controller was active in this test. Furthermore, the peak oxygen uptake achieved in this test was recorded for comparison with values obtained under feedback control.
(4) *Ramp tracking:* The ramp tracking tests allow investigation of the ability of the controllers to follow a linearly increasing target oxygen uptake profile of the kind used in IET in sports physiology. The aim here was to compare the linearity of the feedback-controlled $\dot{V}O_2$ response with the open-loop response, and to assess any differences in the peak $\dot{V}O_2$ value achieved.

3 Results

3.1 Plant model and controller parameters

Based on data obtained from the identification tests, the parameters of the plant model (2) were obtained using linear least squares. The

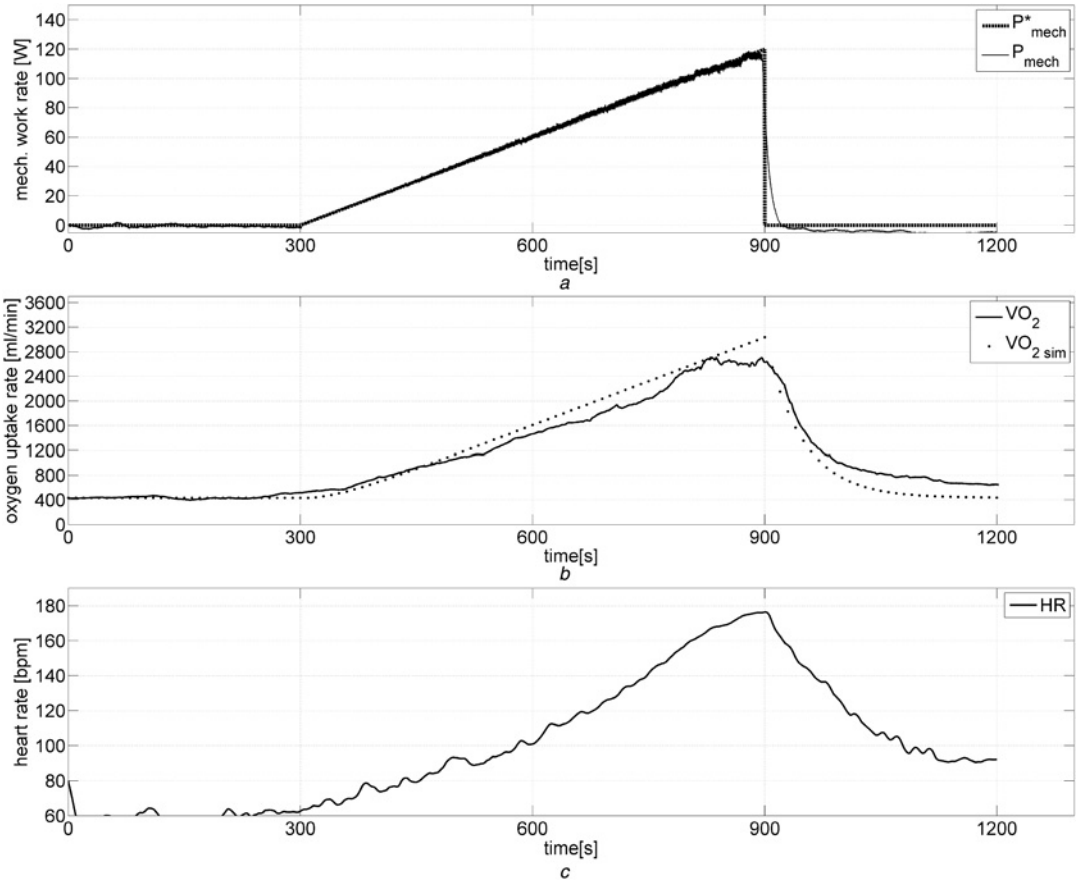

Fig. 7 *Open loop without feedback controller*

a Target mechanical work rate P^*_{mech}, predefined as ramp signal; active mechanical work rate P_{mech} performed by the subject
b Resulting oxygen uptake rate $\dot{V}O_2$ and simulated oxygen uptake rate $\dot{V}O_{2(sim)}$ based on the plant model $P_0(q^{-1})$ and the predefined target mechanical work rate P^*_{mech}
c Heart rate HR

identification procedure led to the choice of a first-order model

$$\dot{V}O_2(t) = \frac{4.4624q^{-1}}{1 - 0.8124q^{-1}} P^*_{\text{mech}}(t) + \frac{1}{\Delta(1 - 0.8124q^{-1})}\, \text{d}\,(t) \tag{7}$$

with d a disturbance term and $\Delta = 1 - q^{-1}$. Following removal of mean signal levels prior to parameter estimation this model conforms with (2). Therefore the nominal transfer function of the plant $P_0(q^{-1})$ is

$$P^*_{\text{mech}} \rightarrow \dot{V}O_2 : P_0(q^{-1}) = \frac{B_0(q^{-1})}{A_0(q^{-1})} = \frac{4.4624q^{-1}}{1 - 0.8124q^{-1}} \tag{8}$$

which has a steady-state gain of 23.8 and a time constant of 48.3 s. The identification data were also used to assess the goodness of fit (73.7%) of this model (Fig. 3*c*). Based on the nominal plant model $P_0(q^{-1})$ and the closed-loop design specifications the two controllers were computed as follows:

$\boldsymbol{C}_1$ – single integrator

$$\begin{aligned} R(q^{-1}) &= 1.0000 - 1.3733q^{-1} + 0.3733q^{-2} \\ S(q^{-1}) &= 0.0332 - 0.0266q^{-1} \\ T(q^{-1}) &= 0.0143 - 0.0078q^{-1} \end{aligned} \tag{9}$$

$\boldsymbol{C}_2$ – double integrator

$$\begin{aligned} R(q^{-1}) &= 1.0000 - 2.4726q^{-1} + 1.9451q^{-2} - 0.4726q^{-3} \\ S(q^{-1}) &= 0.0297 - 0.0515q^{-1} + 0.0223q^{-2} \\ T(q^{-1}) &= 0.0297 - 0.0515q^{-1} + 0.0223q^{-2} \end{aligned} \tag{10}$$

3.2 Step tracking

The results of this test show the ability of the controller C_1 to control the oxygen uptake rate between two levels which are close to the $\dot{V}O_2$ levels observed during the identification tests (Fig. 5*b*). The root mean square error between mechanical work rate and target RMSE($P_{\text{mech}} \leftrightarrow P^*_{\text{mech}}$) is an indicator for the cognitive skills of the subject to perform the human-in-the-loop feedback control, that is, to adapt the effort to the target signal. A very low value of 1.3 W was achieved (Fig. 5*a*). The RMSE($\dot{V}O_2 \leftrightarrow \dot{V}O_{2(\text{sim})}$) of 32 ml/min demonstrates a very good match of $\dot{V}O_2$ and $\dot{V}O_{2(\text{sim})}$ and therefore a proper identification of the plant model P_0. The controller's behaviour matches the theoretical model dynamics with moderately varying target signal output (Fig. 5*b*). Over time, the overall P_{mech} level dropped slightly (Fig. 5*a*) and HR rose because of moderate exertion of the subject (Fig. 5*c*).

3.3 Disturbance rejection

The controller attempts to maintain the constant oxygen uptake signal level (Fig. 6*b*) by adapting the target mechanical work rate (Fig. 6*a*), disturbed by periodical speed level changes (Fig. 6*d*). The RMSE($P_{\text{mech}} \leftrightarrow P^*_{\text{mech}}$) was 1.2 W. The RMSE($\dot{V}O_2 \leftrightarrow \dot{V}O_2^*$) value of 59 ml/min is mainly caused by two major variations, provoked by speed changes. We assume that rising walking speed requires lesser cardiovascular work because the required forces are lower and the gait cycle becomes more efficient. This is indicated by the fact that P^*_{mech} rose (Fig. 6*a*) to maintain the $\dot{V}O_2$ level (Fig. 6*b*). The cardiovascular system reacted less when speed was decreased. Over time, the overall HR level rose slightly (Fig. 6*c*) while $\dot{V}O_2$ and P_{mech} stayed constant (Figs. 6*a* and *b*).

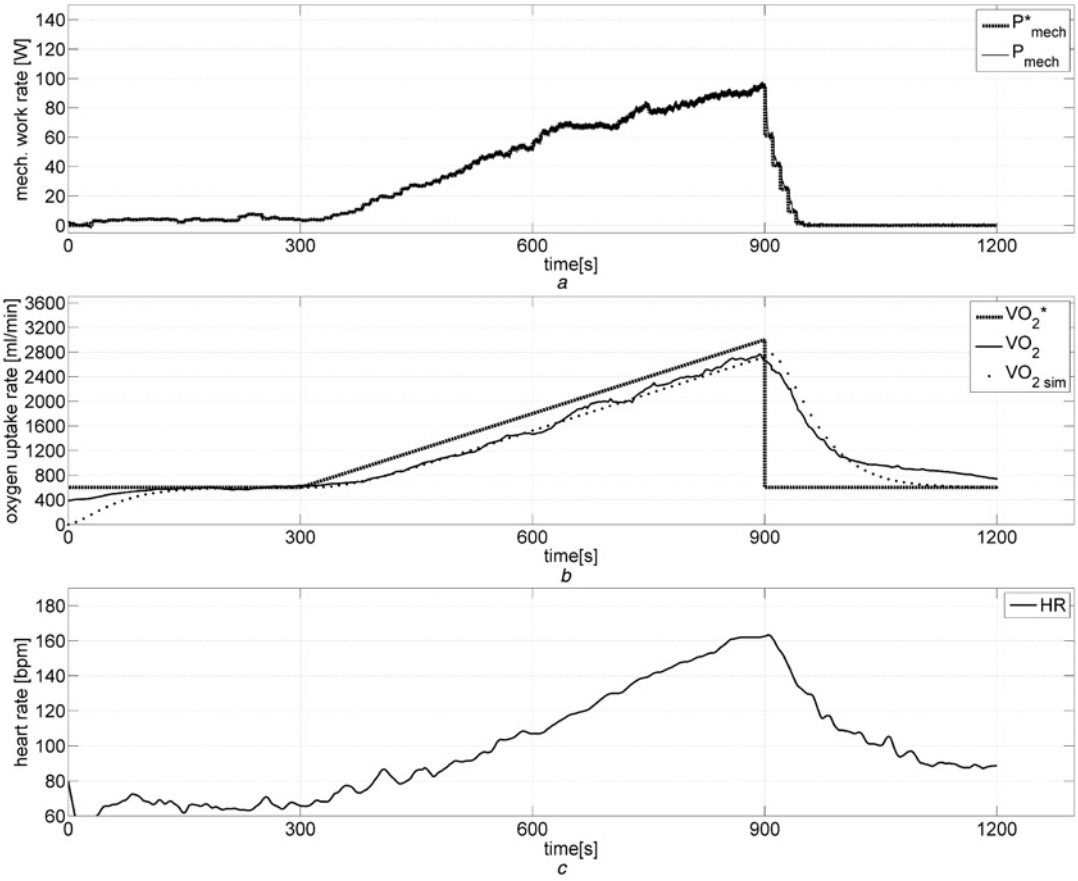

Fig. 8 *Ramp tracking with controller* C_1

a Target mechanical work rate P^*_{mech}, calculated by the controller based on $\dot{V}O_2^*$ and $\dot{V}O_2$; active mechanical work rate P_{mech} performed by the subject
b Target oxygen uptake rate $\dot{V}O_2^*$, oxygen uptake rate $\dot{V}O_2$ and simulated oxygen uptake rate $\dot{V}O_{2(\text{sim})}$ based on the plant model $P_0(q^{-1})$
c Heart rate HR

3.4 Open loop

The open-loop test was performed to investigate the oxygen uptake dynamics without feedback control (Fig. 7). The target mechanical work rate increased linearly to a subject specific peak value ($P_{\text{mech peak}}$) within 10 min (Fig. 7*a*). The test gave a HR_{peak} of 176 bpm, $\dot{V}\text{O}_{2\ \text{peak}}$ of 2600 ml/min and $P_{\text{mech peak}}$ of 120 W. The oxygen uptake rate per work rate relationship ($\dot{V}\text{O}_{2\ \text{peak}}/P_{\text{mech peak}}$) was 21.7 ml/min/W. The non-linearity of the response is clearly visible in $\dot{V}\text{O}_2$ and HR (Figs. 7*b* and *c*). The RMSE($P_{\text{mech}} \leftrightarrow P^*_{\text{mech}}$) value of 2.4 W illustrated the solid cognitive ability of the subject to perform the manual human-in-the-loop feedback control of work rate (Fig. 7*a*). The RMSE($\dot{V}\text{O}_2 \leftrightarrow \dot{V}\text{O}_{2(\text{sim})}$) between the measured $\dot{V}\text{O}_2$ and the linear simulation of $\dot{V}\text{O}_2$ was 174 ml/min which indicates a considerable difference between the non-linear reality of the response and linear first order simulation, thus emphasising the non-linearity. $\dot{V}\text{O}_2$ almost reached a plateau before the end of the ramp (Fig. 7*b*) and HR flattened out (Fig.7*c*).

3.5 Ramp tracking (C_1)

The Ramp tracking with the controller C_1 led to a HR_{peak} of 162 bpm and a $\dot{V}\text{O}_{2\ \text{peak}}$ of 2700 ml/min (Fig. 8*b*). Oxygen uptake rate is clearly below the target of 3000 ml/min (Fig. 8*b*) but higher than in open loop (Fig. 7*b*). The phase lag in the response is expected as a consequence of the single integrator in the controller. $P_{\text{mech peak}}$ was 95 W (Fig. 8*a*) which is a significantly lower value than in the open loop test and therefore the $\dot{V}\text{O}_2$-work rate relationship was 28.4 ml/min/W which is clearly higher. The RMSE($P_{\text{mech}} \leftrightarrow P^*_{\text{mech}}$) was 1.4 W. The RMSE($\dot{V}\text{O}_2 \leftrightarrow \dot{V}\text{O}_{2(\text{sim})}$) of 57 ml/min demonstrated the tracking performance of C_1 (Fig. 8*b*). The work rate signal flattens slightly towards the end of the ramp phase (Fig. 8*a*). The overall response of $\dot{V}\text{O}_2$ in this test is seen to be linear, indicating that the non-linear work rate response is now compensating for the underlying plant non-linearity. HR dynamics (Fig. 8*c*) behave approximately synchronously with the $\dot{V}\text{O}_2$ dynamics.

3.6 Ramp tracking (C_1), delayed

The ramp tracking test with C_1 was repeated with a forward-time-shifted $\dot{V}\text{O}^*_2$ reference signal to extend the ramp phase (Fig. 9*b*), since the phase lag in the ramp response is basically predictable. The test led to a HR_{peak} of 180 bpm and a $\dot{V}\text{O}_{2\ \text{peak}}$ of 2870 ml/min (Figs. 9*b* and *c*). Oxygen uptake rate was clearly higher than in open loop and non-shifted ramp tracking. The HR reached a similar level as in open loop. $P_{\text{mech peak}}$ was 100 W (Fig. 9*a*), still lower than in the open loop test but higher than non-shifted ramp tracking. The $\dot{V}\text{O}_2$-work rate relationship was 29.0 ml/min/W. The RMSE($P_{\text{mech}} \leftrightarrow P^*_{\text{mech}}$) was 2.7 W. The work rate signal flattens clearly in the middle of the ramp phase (Fig. 9*a*, 600 s) while $\dot{V}\text{O}_2$ rises nearly linearly (Fig. 9*b*). The RMSE($\dot{V}\text{O}_2 \leftrightarrow \dot{V}\text{O}_{2(\text{sim})}$) of 117 ml/min reflects the slightly reduced tracking performance of C_1 in this case. This test again illustrates the linearising properties of feedback control of $V\text{O}_2$. The HR has again a similar overall dynamic behaviour as the $\dot{V}\text{O}_2$ (Fig. 9*c*).

3.7 Ramp tracking (C_2)

The ramp tracking test was repeated with the controller C_2 which contains two integrators for zero steady-state error during ramp

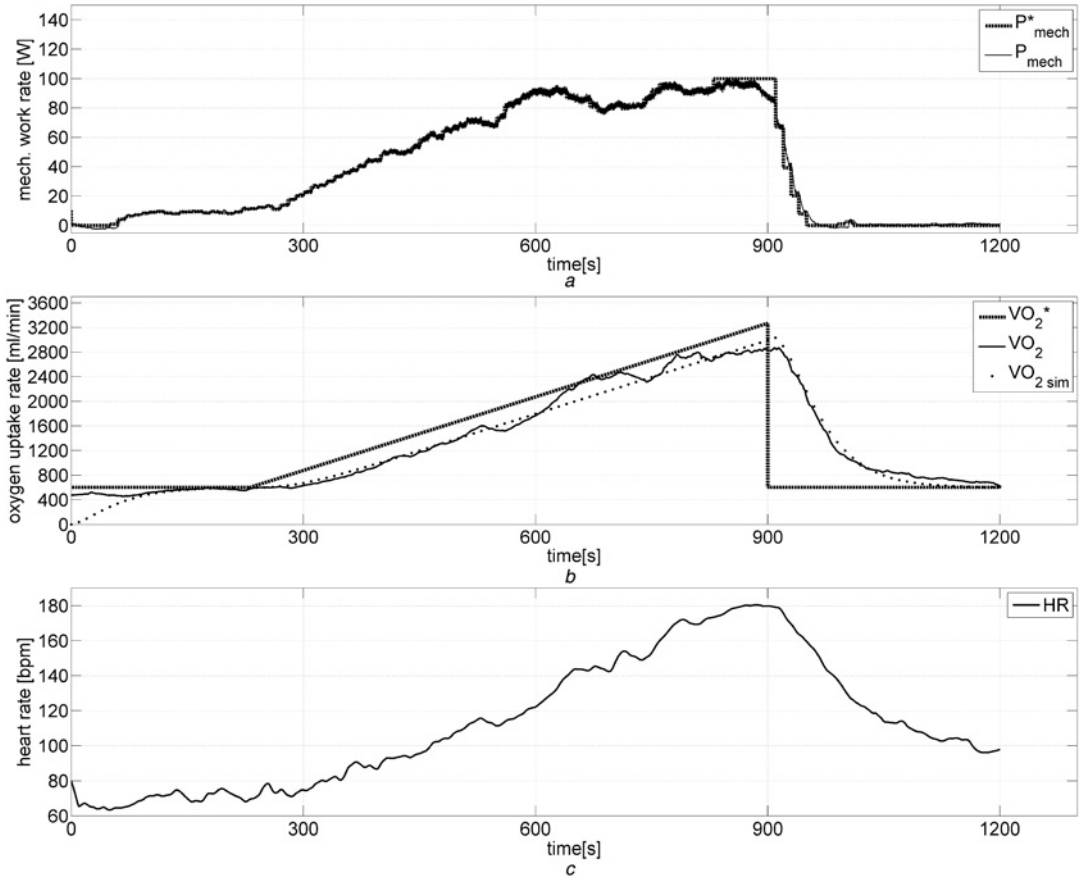

Fig. 9 *Ramp tracking with controller C_1 and a delayed target signal*

a Target mechanical work rate P^*_{mech}, calculated by the controller based on $\dot{V}\text{O}^*_2$ and $\dot{V}\text{O}_2$; active mechanical work rate P_{mech} performed by the subject
b Delayed target oxygen uptake rate $\dot{V}\text{O}^*_2$, oxygen uptake rate $\dot{V}\text{O}_2$ and simulated oxygen uptake rate $\dot{V}\text{O}_{2(\text{sim})}$ based on the plant model $P_0(q^{-1})$
c Heart rate HR

reference tracking (Fig. 10). The RMSE($P_{\text{mech}} \leftrightarrow P^*_{\text{mech}}$) value was 1.6 W. The RMSE($\dot{V}O_2 \leftrightarrow \dot{V}O_{2(\text{sim})}$) of 93 ml/min is similar to the ramp tests with C_1 and confirms the ability of C_2 to track ramps without steady-state error as predicted by simulation (Fig. 10*b*). The test led to a HR_{peak} of 184 bpm, a $\dot{V}O_{2\ peak}$ of 3000 ml/min at $P_{\text{mech peak}}$ of 100 W. The work rate signal flattens continuously (Fig. 10*a*) while $\dot{V}O_2$ rises linearly (Fig. 10*b*), thus emphasising the linearising effects of the feedback compensation. The $\dot{V}O_2$-work rate relationship of 30.0 ml/min/W was slightly higher than in the ramp tests with C_1 and is clearly higher than in open loop. The HR is again in phase with $\dot{V}O_2$ (Fig. 10*c*). The test results are summarised in Fig. 11.

4 Discussion

The aim of this work was to test the technical feasibility of feedback control of oxygen uptake rate during RATE with special focus on ramp tracking. Further, we aimed to investigate the non-linearity of the oxygen uptake response in RATE and the ability of feedback control to linearise this key response. The potential ability of feedback linearisation to promote higher $\dot{V}O_{2\ peak}$ and HR values was examined.

There is lack of aerobic training methods in the field of robotics-based rehabilitation for individuals with neurological deficits. We demonstrated that passive RATE is not intense enough for

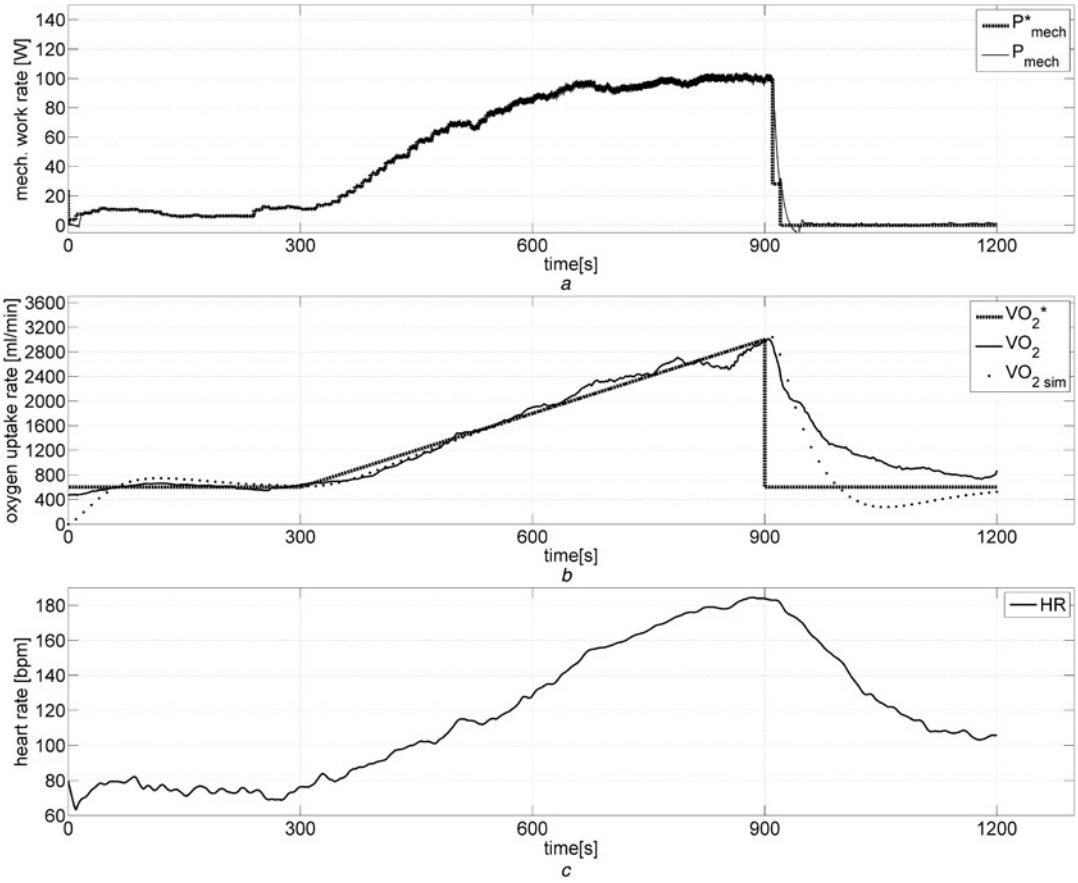

Fig. 10 *Ramp tracking with controller C_2 for compensated tracking delay in ramps*

a Target mechanical work rate P^*_{mech}, calculated by the controller based on $\dot{V}O_2^*$ and $\dot{V}O_2$; active mechanical work rate P_{mech} performed by the subject
b Target oxygen uptake rate $\dot{V}O_2^*$, oxygen uptake rate $\dot{V}O_2$ and simulated oxygen uptake rate $\dot{V}O_{2(\text{sim})}$ based on the plant model $P_0(q^{-1})$
c Heart rate HR

	Step tracking	Disturbance rejection	Open loop	Ramp tracking (C1)	Ramp tracking (C1), delayed	Ramp tracking (C2)
$RMSE(P_{mech} \leftrightarrow P^*_{mech})$	1.3 W	1.2 W	2.4 W	1.4 W	2.7 W	1.6 W
$RMSE(\dot{V}O_2 \leftrightarrow \dot{V}O_{2(sim)})$	32 ml/min		174 ml/min	57 ml/min	117 ml/min	93 ml/min
$RMSE(\dot{V}O_2 \leftrightarrow \dot{V}O_2^*)$		59 ml/min				
$\dot{V}O_{2\ peak}$			2600 ml/min	2700 ml/min	2870 ml/min	3000 ml/min
HR_{peak}			176 bpm	162 bpm	180 bpm	184 bpm
$P_{mech\ peak}$			120 W	95 W	100 W	100 W
$\dot{V}O_{2\ peak}/P_{mech\ peak}$			21.7 ml/min/W	28.4 ml/min/W	29.0 ml/min/W	30.0 ml/min/W

Fig. 11 *Test protocols*

cardiovascular rehabilitation [12] since only 600 ml/min $\dot{V}O_2$ was reached in the passive phase of the identification tests. In the present work, we have demonstrated the technical feasibility of guiding exercise intensity by feedback control of oxygen uptake and as a novelty, also in ramp tracking tasks. The stability of the controllers C_1 and C_2 was seen to be excellent. The single subject was continuously able to precisely follow the moderately varying target mechanical work rate, that is, the controller output, in each test, illustrated by the low RMSE($P_{mech} \leftrightarrow P^*_{mech}$) values between 1.2 and 2.7 W. This result further confirms that the human-in-the-loop feedback structure is technically feasible for mechanical work rate control in RATE in combination with $\dot{V}O_2$ feedback control.

The step tracking test verified the quality of the controller development by demonstrating accurate tracking abilities with a very low RMSE($\dot{V}O_2 \leftrightarrow \dot{V}O_{2(sim)}$) of 32 ml/min, thus confirming previous work [15]. Step tracking for specific $\dot{V}O_2$ profiles may be a promising method for aerobic training [19, 25] in RATE. Patients may perform at a specific, recommended percentage of their maximal aerobic capacity to improve their cardiovascular status.

Increasing speed in the disturbance rejection test led to more efficient gait and less muscle fatigue and therefore to lower $\dot{V}O_2$ values and vice versa since the speed of RATE was lower than the natural self-selected walking speed of around 5 km/h [26–28] which gives the most efficient trade-off between speed and force. Feedback control provides rapid compensation of such disturbances to correct subject-specific oxygen uptake dynamics variations. The resulting RMSE($\dot{V}O_2 \leftrightarrow \dot{V}O^*_2$) value of 59 ml/min illustrates the good performance of the controller C_1 in compensating provoked dynamic changes in $\dot{V}O_2$.

The open loop test clearly illustrates the non-linearity of the $\dot{V}O_2$ (and HR) response during a linear work-rate ramp and therefore the justification for the use of feedback control to obtain a linear oxygen uptake response. Oxygen uptake reached its highest value (2600 ml/min) below the predicted value of 3000 ml/min although the work rate was still rising. The latter rose to the subject's limit of volitional effort. This indicates that peak oxygen uptake during this type of testing is limited by peripheral muscular strength and not by central cardiopulmonary function. The oxygen uptake – work rate relationship was relatively low compared with the feedback controlled ramp tests and indicates non-optimal design for estimation of cardiopulmonary performance parameters. This non-linear behaviour of oxygen uptake is presumably caused by unmeasured components of work which increase disproportionally at higher intensity.

This hypothesis that feedback can linearise the response [21] was experimentally proven in the present work by designing proper feedback controllers and performing ramp tracking tests. The results with the controller C_1 illustrated accurate, but delayed, ramp tracking: the response of oxygen uptake rate was linearised. The phase delay is a predictable property of this type of feedback controller, since C_1 contains only a single integrator. Higher oxygen uptake rates (2700/2870/3000 ml/min) than in open loop (2600 ml/min) were achieved in all feedback-controlled ramp tracking tasks with C_1 and C_2. An important feature and an indicator for the non-linearity of oxygen uptake in RATE is the flattening of the work rate while oxygen uptake rises with constant slope, reflecting the controllers' ability to linearise the response. Work rate final values were on average 20 W lower than in open loop, that is, ∼17% lower muscular effort. A significantly higher $\dot{V}O_2$-work rate relationship resulted. Ramp tracking by feedback seems to be more efficacious for maximal performance testing than open loop tasks because of the well-controlled oxygen uptake slope. Ramp tracking with C_2 resulted in the highest cardiopulmonary values and a completely smooth work rate signal because of the ability to compensate tracking delay using the double integrator in the controller. Ramp tracking with C_1 and a forward-shifted target oxygen uptake signal showed an improvement compared with the non-shifted ramp tracking test. Slightly higher cardiopulmonary values resulted because of the extended ramp phase.

These technical feasibility results suggest there may be significant improvement in measuring $\dot{V}O_{2\,peak}$ values in this type of exercise with feedback control of $\dot{V}O_2$ because of compensation of the non-linear response and a smoother approach to the physiological maximum. The outcomes show that the control approach is robust against changes in the plant dynamics: although plant dynamics change between people and within a given person on different days, all the results obtained here used a single model identified at the start of the experimental series, as described above. The results indicate that higher $\dot{V}O_{2\,peak}$ values may be achieved in RATE with feedback control of $\dot{V}O_2$ because of slower leg fatigue as the load on the subject is lower and the limiting factor is the cardiopulmonary capacity, as desired.

Further work should investigate these hypotheses within a subject cohort to seek consistency and validate our findings. The approach should then be tested in patients where non-linearities and dynamic variabilities are likely to be more pronounced.

5 Conclusion

Feedback control of oxygen uptake rate in RATE is technically feasible for step and ramp tracking tasks in healthy subjects. Non-linearity of the $\dot{V}O_2$ response to linearly increasing open-loop work rate profiles was confirmed and the ability of feedback control to linearise the response was demonstrated. Higher $\dot{V}O_2$-work rate relationships were found in feedback controlled $\dot{V}O_2$ tests, together with higher $\dot{V}O_{2\,peak}$ values. Further work will focus on clinical feasibility and the potential for rehabilitation of the cardiovascular system in patients with neurological deficits.

6 Acknowledgements

We thank Dr Corina Schuster-Amft, head of the research department at Reha Rheinfelden, for provision of laboratory infrastructure.

7 References

1 Galvez J.A., Reinkensmeyer D.J.: 'Robotics for gait training after spinal cord injury', *Top. Spinal Cord Inj. Rehabil.*, 2005, **11**, (2), pp. 18–33
2 Ferris D.P., Sawicki G.S., Domingo A.R.: 'Powered lower limb orthoses for gait rehabilitation', *Top. Spinal Cord Inj. Rehabil.*, 2005, **11**, (2), pp. 34–49
3 Stoller O., de Bruin E.D., Knols R.H., Hunt K.J.: 'Effects of cardiovascular exercise early after stroke: systematic review and meta-analysis', *BMC Neurol.*, 2012, **12**, (1), p. 45
4 Stoller O., Schindelholz M., Bichsel L. *et al.*: 'Feedback-controlled robotics-assisted treadmill exercise to assess and influence aerobic capacity early after stroke: a proof-of-concept study', *Disabil. Rehabil. Assist. Technol.*, 2014, **9**, (4), pp. 271–278
5 Nash M.S., Jacobs P.L., Johnson B.M., Field-Fote E.: 'Metabolic and cardiac responses to robotic-assisted locomotion in motor-complete tetraplegia: a case report', *J. Spinal Cord Med.*, 2004, **27**, (1), pp. 78–82
6 Israel J.F., Campbell D.D., Kahn J.H., Hornby T.G.: 'Metabolic costs and muscle activity patterns during robotic- and therapist-assisted treadmill walking in individuals with incomplete spinal cord injury', *Phys. Ther.*, 2006, **86**, (11), pp. 1466–1478
7 Jack L.P., Purcell M., Allan D.B., Hunt K.J.: 'Comparison of peak cardiopulmonary performance parameters during robotics-assisted treadmill exercise and arm crank ergometry in incomplete spinal cord injury', *Technol. Health Care*, 2010, **18**, (4–5), pp. 285–296
8 Hunt K.J., Jack L.P., Pennycott A., Perret C., Baumberger M., Kakebeeke T.H.: 'Control of work rate-driven exercise facilitates cardiopulmonary training and assessment during robot-assisted gait in incomplete spinal cord injury', *Biomed. Signal Process. Control*, 2008, **3**, (1), pp. 19–28
9 Hunt K.J., Bugmann A.: 'Feedback control of human metabolic work rate during robotics-assisted treadmill exercise', *Biomed. Signal Process. Control*, 2012, **7**, (5), pp. 537–541
10 Chang W.H., Kim M.S., Huh J.P., Lee P.K.W., Kim Y.-H.: 'Effects of robot-assisted gait training on cardiopulmonary fitness in subacute stroke patients: a randomized controlled study', *Neurorehabil. Neural Repair*, 2012, **26**, (4), pp. 318–324
11 Gordon N.F., Gulanick M., Costa F. *et al.*: 'Physical activity and exercise recommendations for stroke survivors – an american heart association scientific statement from the council on clinical cardiology, subcommittee on exercise, cardiac rehabilitation, and prevention; the council on cardiovascular nursing; the council on nutrition, physical activity, and metabolism; and the stroke council', *Circulation*, 2004, **109**, (16), pp. 2031–2041
12 van Nunen M.P.M., Gerrits K.H.L., de Haan A., Janssen T.W.J.: 'Exercise intensity of robot-assisted walking versus overground walking in nonambulatory stroke patients', *J. Rehabil. Res. Dev.*, 2012, **49**, (10), pp. 1537–1546
13 Schindelholz M., Hunt K.J.: 'Feedback control of heart rate during robotics-assisted treadmill exercise', *Technol. Health Care*, 2012, **20**, (3), pp. 179–194

14 Jack L.P., Purcell M., Allan D.B., Hunt K.J.: 'The metabolic cost of passive walking during robotics-assisted treadmill exercise', *Technol. Health Care*, 2011, **19**, (1), pp. 21–27
15 Pennycott A., Hunt K.J., Coupaud S., Allan D.B., Kakebeeke T.H.: 'Feedback control of oxygen uptake during robot-assisted gait', *IEEE Trans. Control Syst. Technol.*, 2010, **18**, (1), pp. 136–142
16 Krewer C., Mueller F., Husemann B., Heller S., Quintern J., Koenig E.: 'The influence of different lokomat walking conditions on the energy expenditure of hemiparetic patients and healthy subjects', *Gait Posture*, 2007, **26**, (3), pp. 372–377
17 Koenig A., Omlin X., Bergmann J., Zimmerli L., Bolliger M., Mueller F., Riener R.: 'Controlling patient participation during robot-assisted gait training', *J. Neuroeng. Rehabil.*, 2011, 8:14
18 Wilmore J.H., Costill D.L.: 'Physiology of sport and exercise' (Human Kinetics, 2004)
19 American College of Sports Medicine: 'Acsm's guidelines for exercise testing and prescription' (Wolters Kluwer/Lippincott Williams & Wilkins Health, 2013, 9th edn.)
20 Wasserman K., Hansen J.E., Sue D.Y., Stringer W.W., Whipp B.J.: 'Principles of exercise testing and interpretation: including pathophysiology and clinical applications' (Lippincott Williams & Wilkins Philadelphia, 1999, 3rd edn.)
21 Hunt K.J., Allan D.B.: 'A stochastic hammerstein model for control of oxygen uptake during robotics-assisted gait', *Int. J. Adaptive Control Signal Process.*, 2009, **23**, (5), pp. 472–484
22 Dunne A.C., Allan D.B., Hunt K.J.: 'Characterisation of oxygen uptake response to linearly increasing work rate during robotics-assisted treadmill exercise in incomplete spinal cord injury', *Biomed. Signal Process. Control*, 2010, **5**, (1), pp. 70–75
23 Schindelholz M., Stoller O., Hunt K.J.: 'A software module for cardiovascular rehabilitation in robotics-assisted treadmill exercise', *Biomed. Signal Process. Control*, 2014, **10**, pp. 296–307
24 Åström K.J., Wittenmark B.: 'Computer-controlled systems: theory and design' (Prentice-Hall, Inc., 1990, 2nd edn.)
25 ATS and ACCP: 'Ats/Accp statement on cardiopulmonary exercise testing', *Am. J. Respir. Crit. Care Med.*, 2003, **167**, (2), pp. 211–277
26 Levine R.V., Norenzayan A.: 'The pace of life in 31 countries', *J. Cross-Cult. Psychol.*, 1999, **30**, (2), pp. 178–205
27 Mohler B.J., Thompson W.B., Creem-Regehr S.H., Pick H.L. Jr., Warren W.H. Jr.: 'Visual flow influences gait transition speed and preferred walking speed', *Exp. Brain Res.*, 2007, **181**, (2), pp. 221–228
28 Browning R.C., Baker E.A., Herron J.A., Kram R.: 'Effects of obesity and sex on the energetic cost and preferred speed of walking', J. Appl. Physiol., 2006, **100**, (2), pp. 390–398